Synthesis, Structure, and Ion Pair Dynamics of β-Diketiminato-Supported Organoscandium Contact Ion Pairs

Paul G. Hayes, Warren E. Piers,* and Masood Parvez

Department of Chemistry, University of Calgary, 2500 University Drive NW, Calgary, Alberta, T2N 1N4, Canada

Received January 4, 2005

A rare family of base-free organoscandium alkyl cations stabilized by β-diketiminato ligands (Ar)NC(R)CHC(R)N(Ar) (Ar = 2,6-^{i}Pr-C_6H_3; R = CH_3 (L^{Me}), R = ^{t}Bu (L^{tBu})) has been prepared by reaction of $LScR_2$ with perfluorinated boranes $B(C_6F_5)_3$ and $(C_{12}F_8)B(C_6F_5)$. While the L^{Me} ancillary lacked sufficient steric bulk to prevent C_6F_5 transfer to the metal center, the L^{tBu} derivatives were quite robust in solution. Although these species were subject to thermal decomposition via metalation of an isopropyl group and loss of RH ($\Delta S^{\ddagger} = -7.0(7)$ eu and $\Delta H^{\ddagger} = 21.5(2)$ kcal mol^{-1}), the process was not sufficiently rapid to hinder the development of their rich organometallic chemistry. The solution and solid state structures were studied in detail, revealing the presence of both *exo*- and *endo*-$MeB(Ar^F)_3$ isomers if the metal alkyl was small. Detailed NMR studies (low-temperature EXSY) allowed for observation of both inter- and intramolecular ion pair reorganization processes, whose mechanism is discussed in terms of the involvement of "solvent separated ion pairs". This is the first such study involving non-metallocenium group 3 metal based ion pairs.

Introduction

Organometallic cations of the early transition metals, particularly those of group 4, have been studied intensively over the past couple of decades due to their importance as catalytic species in a variety of reactions, including olefin polymerization,[1] C−H bond functionalization,[2] and Si−H dehydropolymerization.[3] Generally these cations are formed via reaction of neutral organometallic precursors with strong Lewis acids such as perfluoroarylboranes,[4] or trityl salts of weakly coordinating anions.[5] The static structural features of many of these ion pairs are well established,[2,6] but debate concerning the dynamic behavior of these species in solution, processes that have important consequences for catalyst behavior in the polymerization reactions mentioned above,[7] has been lively.

Trends in the rates of exchange of diastereotopic groups on the supporting ligand framework and the activation parameters associated with the process(es) involved have been used to infer mechanistic information concerning the nature of the dynamic behavior associated with group 4 metallocenium ion pairs. For example, Marks et al. have developed an elegant 1,1′,2,2′-tetramethylzirconocene probe to characterize two dynamic processes within ion pairs incorporating the $[H_3CB(C_6F_5)_3]^-$ anion.[6] The first exchanges both the diastereotopic ring methyl groups and the abstracted B-CH_3/nonabstracted Zr-CH_3 pair via "$B(C_6F_5)_3$ dissociation/reabstraction" (Scheme 1). The second process, referred to as "ion pair symmetrization", involves dissociation of the entire methylborate anion from the contact ion pair (CIP), possibly into a solvent-separated ion pair (SSIP), followed by recombination on the other side of the zirconocene wedge. This process exchanges only the diastereotopic ring methyl groups and not the Zr-Me/B-Me pair.

Similar exchange phenomena have been examined in metallocenium ions with other ligand sets featuring diastereotopic groups[8−10] such that a range of data concerning these processes is available. The intimate details of the mechanisms of the two processes are profoundly influenced by variables such as metallocenium ion structure, solvent/medium polarity and ionic strength, the concentration regime employed, and the stoichiometry of the ion pair generating reaction.[11] Furthermore, the role of ion pair aggregates in this

* To whom correspondence should be addressed. E-mail: wpiers@ucalgary.ca.

(1) Chen, E. Y. X.; Marks, T. J. *Chem. Rev.* **2000**, *100*, 1391.

(2) (a) Jordan, R. F.; Taylor, D. F. *J. Am. Chem. Soc.* **1989**, *111*, 778. (b) Rodewald, S.; Jordan, R. F. *J. Am. Chem. Soc.* **1994**, *116*, 4491.

(3) (a) Sadow, A. D.; Tilley, T. D. *Organometallics* **2001**, *20*, 4457. (b) Sadow, A. D.; Tilley, T. D. *Organometallics* **2003**, *22*, 3577. (c) Sadow, A. D.; Tilley, T. D. *J. Am. Chem. Soc.* **2003**, *125*, 9462.

(4) (a) Yang, X. M.; Stern, C. L.; Marks, T. J. *J. Am. Chem. Soc.* **1991**, *113*, 3623. (b) Ewen, J. A.; Elder, M. J. *CA-A* **1991**, *2*, 27. (c) Ewen, J. A.; Elder, M. J. *Chem. Abstr.* **1991**, *115*, 136998g; 256895t. (d) Hlatky, G. G.; Turner, H. W. In PCT Int. Appl. W/O 91/14713; Exxon Chemical Co., 1991. (e) Piers, W. E. *Adv. Organomet. Chem.* **2005**, *52*, 1.

(5) Chien, J. C. W.; Rausch, M. D.; Tsai, W.-M. *J. Am. Chem. Soc.* **1991**, *113*, 8570.

(6) Yang, X. M.; Stern, C. L.; Marks, T. J. *J. Am. Chem. Soc.* **1994**, *116*, 10015.

(7) See: Chen, M.-C.; Roberts, J. A. S.; Marks, T. J. *J. Am. Chem. Soc.* **2004**, *126*, 4605, and references therein.

(8) (a) Beck, S.; Geyer, A.; Brintzinger, H.-H. *Chem. Commun.* **1999**, 2477. (b) Beck, S.; Lieber, S.; Schaper, F.; Geyer, A.; Brintzinger, H.-H. *J. Am. Chem. Soc.* **2001**, *123*, 1483. (c) Schaper, F.; Geyer, A.; Brintzinger, H. H. *Organometallics* **2002**, *21*, 473.

(9) Mohammed, M.; Nele, M.; Al-Humydi, A.; Xin, S.; Stapleton, R. A.; Collins, S. *J. Am. Chem. Soc.* **2003**, *125*, 7930.

(10) Song, F.; Cannon, R. D.; Bochmann, M. *J. Am. Chem. Soc.* **2003**, *125*, 7641.

10.1021/om050007v CCC: $30.25
Publication on Web 02/16/2005

Scheme 1

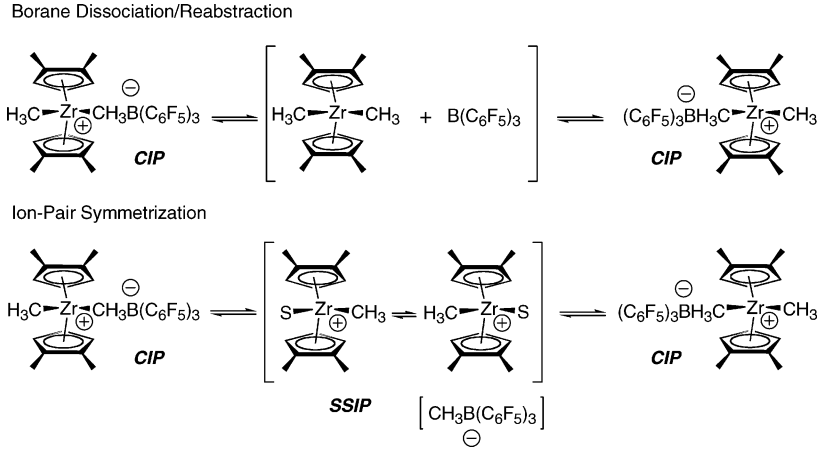

exchange process has been debated and probed by a variety of sophisticated NMR techniques, including EXSY (exchange spectroscopy) and 1D DPFGSE-NOE (differential pulse field gradient spin−echo nuclear Overhauser effect) experiments.[12] The picture that accrues from these studies is that in the less polarized CIPs, or "inner sphere ion pairs",[12b] no evidence for ion pair aggregation is found even at relatively high concentrations, while for more charge-separated SSIPs ("outer sphere ion pairs") aggregation into ion pair quadruples (or multiples) is substantial at concentrations as low as 1−2 mM, which is substantially higher than the concentrations typically employed in industrially relevant olefin polymerization processes. Nevertheless, such aggregates might be expected to play a role in the observed ion pair reorganization processes in metallocenium ions, and while explicit evidence for the role of such aggregates in ion pair reorganization processes has been lacking, it is clear from the above studies[12b] that significantly greater ion mobility is to be expected in the SSIPs than the CIPs, in which fairly strong anion−cation interactions are featured.

In contrast to the extensive developments concerning the group 4 metal organometallic cations, fewer examples of cations based on the group 3 or lanthanide metals have been presented, and even less is known about their dynamic behavior.[13] Metallocenium ions of the group 3 metals of general formula $[Cp_2M^{III}]^+[A]^-$ have been prepared[14] and function as models for weak cation−anion or cation−solvent interactions, but of course do not retain a reactive alkyl group. Thus, to develop the chemistry of well-defined alkyl cations of group 3 metals, a monoanionic supporting ligand of sufficient steric bulk is required; examples of suitable ligands have only recently emerged, allowing for detailed study of this family of compounds,[15] but even in these instances, few are free of coordinating bases. Interest in such cations stems from the presumption that they would exhibit the same boost in reactivity that group 4 metal-based cations display in comparison to their neutral counterparts. Several recent publications have proven this to be the case; where direct comparison is possible, cationic group 3 compounds show both increased activity and novel selectivity in, for example, scandium-catalyzed ethylene/olefin copolymerizations,[15a] olefin and alkyne hydroaminations,[16] or alkyne dimerizations.[15b]

Our group has exploited the bulky β-diketiminato ligand framework, an ancillary ligand that has gained considerable importance over the past decade,[17] to stabilize a variety of base-free dialkyl organoscandium compounds.[18,19] The ligand incorporating methyl groups in the diketimine backbone is slightly less sterically bulky than the ^{t}Bu-substituted version, but both can support formally eight-electron dialkyl complexes that adopt the out-of-plane structure shown in **I**. This

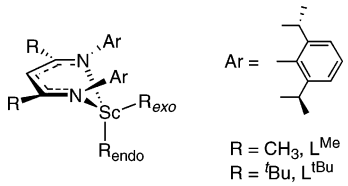

I

engenders diastereotopicity in the Sc-R groups, as well as the N-Ar substituents in the slow exchange limiting structure, but exchange of the diastereotopic groups is rapid on the NMR time scale. Furthermore, in the CIPs

(11) (a) Deck, P. A.; Marks, T. J. *J. Am. Chem. Soc.* **1995**, *117*, 6128. (b) Deck, P. A.; Beswick, C. L.; Marks, T. J. *J. Am. Chem. Soc.* **1998**, *120*, 1772. (c) Beswick, C. L.; Marks, T. J. *Organometallics* **1999**, *18*, 2410. (d) Beswick, C. L.; Marks, T. J. *J. Am. Chem. Soc.* **2000**, *122*, 10358.

(12) (a) Stahl, N. G.; Zuccaccia, C.; Jensen, T. R.; Marks, T. J. *J. Am. Chem. Soc.* **2003**, *125*, 5256. (b) Zuccaccia, C.; Stahl, N. G.; Macchiono, A.; Chen, M.-C.; Roberts, J. A.; Marks, T. J. *J. Am. Chem. Soc.* **2004**, *126*, 1448.

(13) Piers, W. E.; Emslie, D. J. H. *Coord. Chem. Rev.* **2002**, *233−234*, 131.

(14) (a) Hazin, P. N.; Bruno, J. W.; Schulte, G. K. *Organometallics* **1990**, *9*, 410. (b) Bouwkamp, M. W. Ph.D. Thesis, University of Groningen, 2004.

(15) (a) Bambirra, S.; Bouwkamp, M. W.; Meetsma, A.; Hessen, B. *J. Am. Chem. Soc.* **2004**, *126*, 9182. (b) Tazelaar, C. G. J.; Bambirra, S.; van Leusen, D.; Meetsma, A.; Hessen, B.; Teuben, J. H. *Organometallics* **2004**, *23*, 936. (c) Bambirra, S.; van Leusen, D.; Meetsma, A.; Hessen, B.; Teuben, J. H. *Chem. Commun.* **2001**, 637. (d) Arndt, S.; Zeimentz, P. M.; Spaniol, T. P.; Okuda, J.; Honda, M.; Tatsumi, K. *Dalton Trans.* **2003**, 3622. (e) Arndt, S.; Spaniol, T. P.; Okuda, J. *Organometallics* **2003**, *22*, 775. (f) Arndt, S.; Spaniol, T. P.; Okuda, J. *Chem. Commun.* **2002**, 896. (g) Cameron, T. M.; Gordon, J. C.; Michalczyk, R.; Scott, B. L. *Chem. Commun.* **2003**, 2282. (h) Schaverien, C. J. *Organometallics* **1992**, *11*, 3476. (i) Hajela, S.; Schaefer, W. P.; Bercaw, J. E. *J. Organomet. Chem.* **1997**, *532*, 45. (j) Hayes, P. G.; Welch, G. C.; Emslie, D. J. H.; Noack, C. L.; Piers, W. E.; Parvez, M. *Organometallics* **2003**, *22*, 1577. (k) Lawrence, S. C.; Ward, B. D.; Dubberley, S. R.; Kozak, C. M.; Mountford, P. *Chem. Commun.* **2003**, 2880.

(16) Lauterwasser, F.; Hayes, P. G.; Piers, W. E.; Brase, S.; Schafer, L. L. *Organometallics* **2004**, *23*, 2234.

Scheme 2

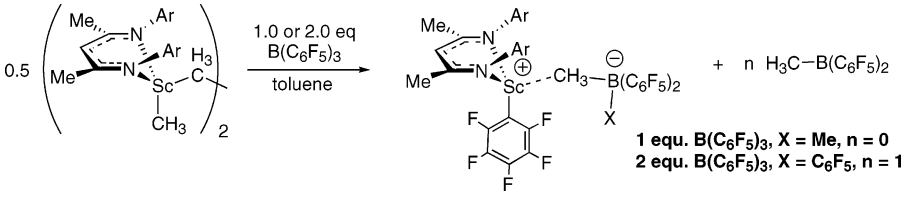

generated from these neutral dialkyls and $B(C_6F_5)_3$,[20] which are highly active olefin polymerization catalysts, this exchange phenomenon can be used to probe the ion pair dynamic processes associated with these non-metallocene ion pairs. Herein we fully describe the synthesis and properties of these CIPs along with their dynamic behavior in toluene solution.

Results and Discussion

Reactions of $[L^{Me}ScMe_2]_2$ and $L^{tBu}ScMe_2$ with $B(C_6F_5)_3$. Reaction of dimeric $[L^{Me}ScMe_2]_2$[21] with 1 equiv of $B(C_6F_5)_3$ in toluene at −35 °C afforded the expected ion pair $[L^{Me}ScMe]^+[MeB(C_6F_5)_3]^-$ as monitored by ^1H, ^{11}B, and ^{19}F NMR spectroscopy. A broad resonance at −16.8 ppm in the ^{11}B NMR spectrum, in combination with a $\Delta\delta_{m,p} = 4.2$ ppm in the ^{19}F NMR spectrum, supported the formation of a loosely bound CIP with a μ-methyl contact between the boron and scandium centers.[22] While the ion pair was stable at −35 °C, upon gradual warming to room temperature, $-C_6F_5$ transfer from the borate to scandium generated the ion pair $[L^{Me}Sc(C_6F_5)]^+[Me_2B(C_6F_5)_2]^-$ (Scheme 2) presumably via the neutral complex $L^{Me}Sc(Me)(C_6F_5)$ and $MeB(C_6F_5)_2$.[23] This ion pair was highly soluble in toluene and thermally unstable at ambient temperature and so was characterized only in solution. However, a more robust ion pair incorporating $[MeB(C_6F_5)_3]^-$ instead of the $[Me_2B(C_6F_5)_2]^-$ anion was isolated when 2 equiv of $B(C_6F_5)_3$ was employed; here, the initial product was the dicationic species $[L^{Me}Sc]^{2+}[MeB(C_6F_5)_3]^-{}_2$, as evidenced by the disappearance of both Sc-CH_3 resonances in the ^1H NMR spectrum and the emergence of two sets of $[MeB(C_6F_5)_3]^-$ signals in the ^{19}F NMR spectrum. This doubly activated species[24] is also prone to C_6F_5 transfer, ultimately giving rise to *endo*-$[L^{Me}Sc(C_6F_5)]^+[MeB(C_6F_5)_3]^-$ (Scheme 2),[25] which was characterized by X-ray crystallography (Figure 1).

The solid state structure of *endo*-$[L^{Me}Sc(C_6F_5)]^+[MeB(C_6F_5)_3]^-$ exhibits a symmetrically bound β-diketiminato ancillary with the metal lying 0.645(5) Å from the plane formed by the C_3N_2 ligand backbone. An elongated Sc−C1 distance of 2.699(4) Å (cf. an average Sc−C distance of 2.29 Å in $[L^{Me}ScMe_2]_2$) is indicative of a weakly coordinating $[MeB(C_6F_5)_3]^-$ anion. The nonlinear Sc−C1−B angle of 133.42(25)° is atypical of metallocenium ion pairs with this counteranion,[1] but this bending allows for an interaction between Sc and F1, as evidenced by a short contact of 2.221(2) Å.[26] This dative distance is comparable to those observed in $[L^{tBu}ScMe]^+[MeB(C_6F_5)_3]^-$ (2.390(4) Å)[20b] and $[Cp^*_2Sc(FC_6H_5)_2]^+[BPh_4]^-$ (2.2725(17), 2.2884(16) Å),[14b] but longer than the bridging Sc−F distances (2.039(23)−2.070(24) Å) found in $[Cp_2ScF]_3$.[27] The C33−F1 bond distance of 1.413(5) Å is concomitantly elongated relative to the other noncoordinating C−F bonds, which average to 1.349(5) Å; the remaining Sc−C and Sc−N distances agree well with typical values.

The low-temperature ^1H and ^{19}F NMR spectra of $[L^{Me}Sc(C_6F_5)]^+[MeB(C_6F_5)_3]^-$ do not indicate a solution structure consistent with that observed by X-ray crys-

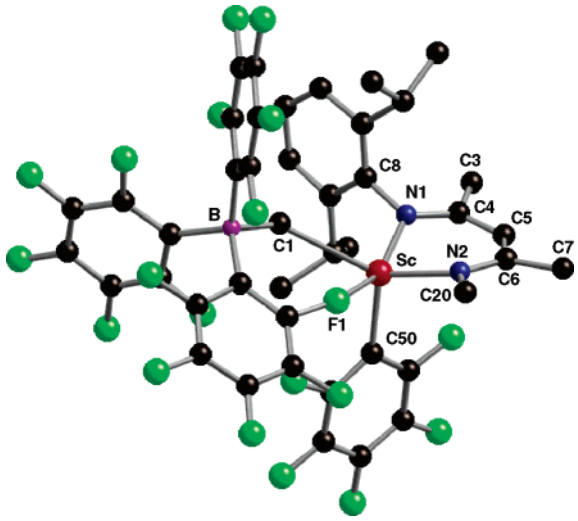

Figure 1. Crystalmaker depiction of the molecular structure of *endo*-$[L^{Me}Sc(C_6F_5)]^+[MeB(C_6F_5)_3]^-$. Hydrogen atoms and all of the atoms of the front *N*-aryl group (except for *ipso*-C(20)) are removed for clarity. Selected bond distances (Å): Sc−N(1), 2.094(3); Sc−N(2), 2.087(3); Sc−C(1), 2.699(4); Sc−C(50), 2.220(5); Sc−F(1), 2.221(2). Selected bond angles (deg): N(1)−Sc−N(2), 87.9(3); Sc−C(1)−B, 133.4(2); C(1)−Sc−C(50), 111.7(2).

(17) Bourget-Merle, L.; Lappert, M. F.; Severn, J. R. *Chem. Rev.* **2002**, *102*, 3031.
(18) (a) Hayes, P. G.; Piers, W. E.; Lee, L. W. M.; Knight, L. K.; Parvez, M.; Elsegood, M. R. J.; Clegg, W. *Organometallics* **2001**, 20, 2533. (b) Knight, L. K.; Piers, W. E.; McDonald, R. *Chem. Eur. J.* **2000**, *6*, 4322. (c) Knight, L. K.; Piers, W. E.; Fleurat-Lessard, P.; McDonald, R.; Parvez, M. *Organometallics* **2004**, *23*, 2087.
(19) Other scandium β-diketiminato complexes: (a) Basuli, F.; Tomaszewski, J.; Huffman, J. C.; Mindiola, D. J. *Organometallics* **2003**, *22*, 4705. (b) Neculai, A. M.; Neculai, D.; Roesky, H. W.; Magull, J.; Baldus, M.; Andronesi, O.; Jansen, M. *Organometallics* **2002**, *21*, 2590.
(20) (a) Lee, L. W. M.; Piers, W. E.; Elsegood, M. R. J.; Clegg, W.; Parvez, M. *Organometallics* **1999**, *18*, 2947. (b) Hayes, P. G.; Piers, W. E.; McDonald, R. *J. Am. Chem. Soc.* **2002**, *124*, 2132.
(21) Hayes, P. G.; Piers, W. E.; Parvez, M. *J. Am. Chem. Soc.* **2003**, *125*, 5622.
(22) Horton, A. D. *Organometallics* **1996**, *15*, 2675.
(23) Identified by ^1H NMR spectroscopy: Spence R. E. v H.; Piers, W. E.; Sun, Y.; Parvez, M.; MacGillivray, L. R.; Zaworotko, M. J. *Organometallics* **1998**, *17*, 2459.
(24) Guérin, F.; Stephan, D. W. *Angew. Chem., Int. Ed.* **2000**, 39, 1298.
(25) Because the scandium center deviates from the β-diketiminato ligand plane in these complexes, the two remaining ligand coordination sites are diastereotopic. We refer to the site pointing away from the C_3N_2 framework as the *exo* position and that situated underneath the C_3N_2 ring as the *endo* site. In the CIPs discussed herein, we refer to *exo* and *endo* isomers as those with the remaining alkyl group in this position.
(26) Song, X.; Thornton-Pett, M.; Bochmann, M. *Organometallics* **1998**, *17*, 1004.
(27) Bottomley, F.; Paez, D. E.; White, P. S. *J. Organomet. Chem.* **1985**, *291*, 35.

Scheme 3

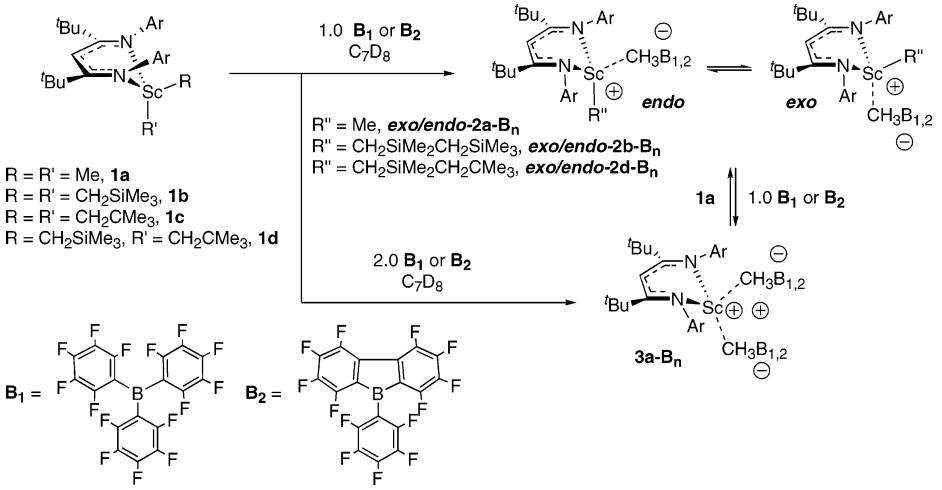

tallography; there are no upfield resonances[28] pointing to an Sc−F interaction in the low temperature (−100 °C) ^{19}F NMR spectrum. Rather, two isomers are observed in a 7:3 ratio, corresponding to the diastereomers in which the $-C_6F_5$ group occupies the *endo* or *exo* positions.[29]

Pentafluorophenyl group transfer from the $[H_3CB(C_6F_5)_3]^-$ anion to sterically accessible electrophilic centers has been observed in several other cases.[30] Since this is essentially an undesirable deactivation pathway in the context of olefin polymerization, we turned to the more sterically encumbered scandium dialkyl cations supported by the L$^{t\mathrm{Bu}}$ ligand in hopes of disfavoring this reaction path. As reported previously,[20b] the CIPs obtained via reaction of the monomeric dimethyl compound L$^{t\mathrm{Bu}}$ScMe$_2$, **1a**, and 1 or 2 equiv of $B(C_6F_5)_3$ (henceforth referred to as $\mathbf{B_1}$) are immune to $-C_6F_5$ transfer under ambient conditions, due to the greater steric congestion provided by this ligand in comparison to L$^{\mathrm{Me}}$, and form well-behaved ion pairs (Scheme 3). Thus, the mono methyl ion pair $\mathbf{2a}-\mathbf{B_1}$ is formed as a stable, isolable yellow solid, and its structure has been determined by X-ray crystallography. As in the case of the *endo*-$[L^{\mathrm{Me}}Sc(C_6F_5)]^+[MeB(C_6F_5)_3]^-$ ion pair discussed above, the isomer $\mathbf{2a}-\mathbf{B_1}$ that crystallizes is the *endo* isomer,[20b] in which the bulky $[H_3CB(C_6F_5)_3]^-$ anion occupies the *exo* site via a similar coordination mode featuring a C-F → Sc interaction.[20b] Ion pair $\mathbf{2a}-\mathbf{B_1}$ is stable in toluene for prolonged periods below 0 °C and indefinitely as a solid under an inert atmosphere if stored at −35 °C. Although no sign of decomposition via C_6F_5 transfer occurred upon warming to room temperature, $\mathbf{2a}-\mathbf{B_1}$ slowly evolved methane through a metalation pathway involving a methyl C−H bond of one of the *N*-aryl isopropyl groups, similar to that observed for the neutral dialkyl species (vide infra).

Further activation of this cation is observed when a second equivalent of $\mathbf{B_1}$ is added, forming the unusual dication $\mathbf{3a}-\mathbf{B_1}$ as a pale yellow solid; treatment of this species with 1 equiv of neutral dimethyl complex **1a** regenerates the monomethyl cation $\mathbf{2a}-\mathbf{B_1}$. Such "double activation" reactions are rare, but have precedence in group 4 metal systems with strongly donating ligands.[24] The solution ^{1}H NMR data for $\mathbf{3a}-\mathbf{B_1}$ were diagnostic, with no Sc-Me resonances in evidence and two distinct $[MeB(C_6F_5)_3]^-$ signals at 1.55 and 1.92 ppm for the chemically diastereotopic *exo* and *endo* anions. The ^{19}F NMR spectrum also exhibited two sets of C_6F_5 resonances with $\Delta\delta_{m,p} = 4.3$ and 5.8 ppm (assigned by ^{19}F−^{19}F 2D COSY). These values correlate well with those observed for the two isomers of $\mathbf{2a}-\mathbf{B_1}$. While a ^{19}F−^{19}F 2D EXSY experiment confirmed the two anions are exchanging, it was not possible to coalesce the process in one-dimensional ^{1}H NMR experiments.

As is also shown in Scheme 3, all of the above chemistry can be repeated using the similarly Lewis acidic perfluoro-9-borafluorene species $(C_{12}F_8)B(C_6F_5)$, $\mathbf{B_2}$.[31] Analogous products $\mathbf{2a}-\mathbf{B_2}$ and the doubly activated dication $\mathbf{3a}-\mathbf{B_2}$ were formed and exhibited essentially the same properties as the closely related $\mathbf{B_1}$ series. These ion pairs were prepared for use in the ion pair dynamic studies described below.

Because the two substituents associated with the scandium center in ion pairs $\mathbf{2a}-\mathbf{B}_n$ are different, these compounds exist in solution as an exchanging pair of diastereomers, which are indistinguishable by ^{1}H or ^{19}F NMR spectroscopy at room temperature. However, as samples of $\mathbf{2a}-\mathbf{B}_n$ are cooled, coalescence behavior is observed in the ^{1}H and ^{19}F NMR spectra, and the exchange is frozen out to reveal spectra consistent with the presence of *exo* and *endo* isomers in a 2.2:1 ratio as shown in Scheme 3 and the representative ^{1}H NMR spectra for $\mathbf{2a}-\mathbf{B_1}$ in Figure 2. The barrier to exchange between the two diastereomers was estimated to be 12.4(5) kcal mol^{-1} based on analysis of the coalescence behavior of the spectra, a barrier comparable to those observed for exchange of *endo* and *exo* alkyl groups in the neutral dialkyl compounds. As will be seen, the observed exchange between ***endo*-2a**$-\mathbf{B_1}$and ***exo*-2a**−

(28) (a) Ruwwe, J.; Erker, G.; Fröhlich, R. *Angew. Chem., Int. Ed. Engl.* **1996**, *35*, 80. (b) Temme, B.; Karl, J.; Erker, G. *Chem. Eur. J.* **1996**, *2*, 919. (c) Temme, B.; Erker, G.; Karl, J.; Luftmann, H.; Fröhlich, R.; Kotila, S. *Angew. Chem., Int. Ed. Engl.* **1995**, *34*, 1755.

(29) The assignment of isomers was not rigorously established in this case.

(30) (a) Korolev, A. V.; Ihara, E.; Guzei, I. A.; Young, V. G., Jr.; Jordan, R. F. *J. Am. Chem. Soc.* **2001**, *123*, 8291. (b) Spitzmesser, S. K.; Gibson, V. C. *J. Organomet. Chem.* **2003**, *673*, 95. (c) Walker, D. A.; Woodman, T. J.; Hughes, D. L.; Bochmann, M. *Organometallics* **2001**, *20*, 3772. (d) Walker, D. A.; Woodman, T. J.; Schormann, M.; Hughes, D. L.; Bochmann, M. *Organometallics* **2003**, *22*, 797.

(31) Chase, P. A.; Piers, W. E.; Patrick, B. O. *J. Am. Chem. Soc.* **2000**, *122*, 12911.

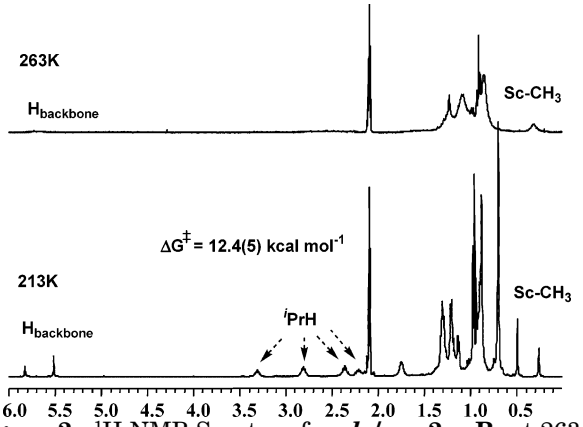

Figure 2. ^{1}H NMR Spectra of ***endo/exo*-2a**−**B$_1$** at 263 K (near coalescence, top) and 213 K (slow exchange regime, bottom).

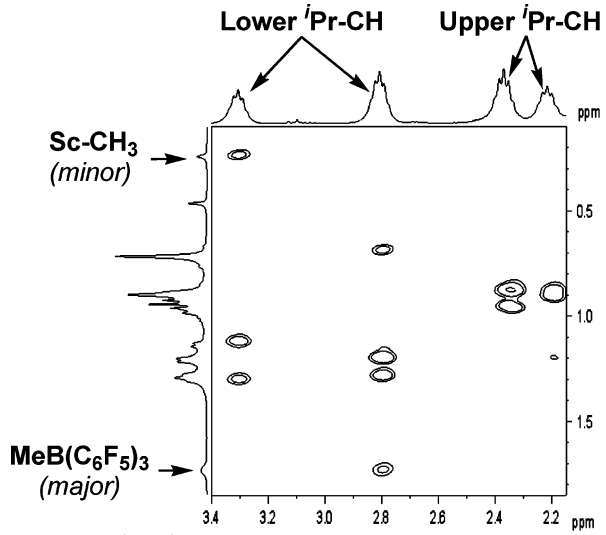

Figure 3. ^{1}H−^{1}H 2D ROESY NMR spectrum of ***endo/exo*-2b**−**B$_1$**.

B$_1$ offers an opportunity to probe the ion pair dynamics in these non-metallocene ion pairs.

As in the case of $[L^{Me}Sc(C_6F_5)]^+[MeB(C_6F_5)_3]^-$, no evidence for the $[(\mu\text{-}CH_3)(\mu\text{-}FC_6F_4)B(C_6F_5)_2]^-$ bonding mode of the methylborate anion was observed in solution, suggesting that the normal μ-CH_3 mode, in which a more or less linear Sc−C−B arrangement occurs, is predominant in solution. When the sample of Figure 2 was analyzed via a ^{1}H−^{1}H 2D-ROESY NMR experiment,[32] distinct cross-peaks were observed between one of the major isomer isopropyl methine groups and the B-CH_3 group and a minor isomer isopropyl resonance and the Sc-CH_3 signal (Figure 3). On the basis of an analysis of the solid state structures of several scandium β-diketiminato derivatives, the Sc-C_{endo} carbon atom is closest to the lower isopropyl methine carbons, as illustrated in **II**. The Sc-C_{exo} carbon is invariably further

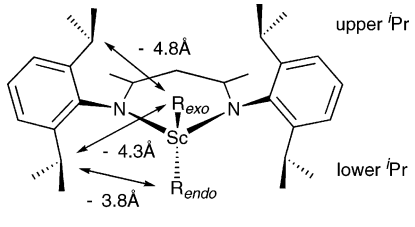

II

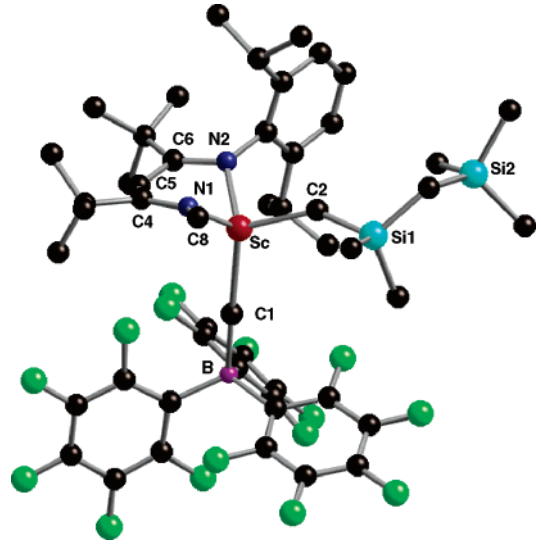

Figure 4. Crystalmaker depiction of ***exo*-2b**−**B$_1$**. Hydrogen atoms and all atoms of the front *N*-aryl group (except for *ipso*-C(8)) are removed for clarity. Selected bond distances (Å): Sc−N(1), 2.072(2); Sc−N(2), 2.086(2); Sc−C(1), 2.499(2); Sc−C(2), 2.133(3). Selected bond angles (deg): N(1)−Sc−N(2), 96.65(7); Sc−C(1)−B, 176.8(2); C(1)−Sc−C(2), 113.5(1); Sc−C(2)−Si(1), 144.5(2).

removed from these isopropyl groups by ∼0.5 Å, while the upper isopropyl methine carbons are even further away at ∼4.8 Å. We thus tentatively assign the major solution isomer as ***exo*-2a**−**B$_1$** and the minor diastereoisomer as the ***endo*-2a**−**B$_1$** even though the compound crystallizes preferentially as the ***endo*-2a**−**B$_1$** structure.[33] We attribute this observation to the fact that the bonding mode of the anion in the solid is different from that observed in solution.

The boranes **B$_1$** and **B$_2$** also react rapidly with the bis(trimethylsilylmethyl) organoscandium complex **1b**[18a] to give ion pairs **2b**−**B$_n$**, in which the two silyl alkyl groups have coupled, and the counteranion is again the methylborate species $[H_3CB(C_6F_5)_3]^-$. This reaction path was indicated by the pattern of three resonances upfield of 0 ppm in a 9:6:2 ratio observed in the ^{1}H NMR spectrum of **2b**−**B$_1$** in d_8-toluene. In addition, a broad peak, integrating for 3H, was observed at 1.51 ppm, the region where the methylborate signals in the previously generated ion pairs are found. Interestingly, and unlike ion pairs **2a**, the **2b** ion pairs exist as only one diastereoisomer at all temperatures, as determined by ^{1}H, ^{11}B, and ^{19}F NMR spectroscopy; furthermore, reaction with a second equivalent of borane is not observed in this case. An X-ray diffraction structure determination showed this to be the *exo* isomer (Figure 4). Crystals of this ion pair were grown from cold hexanes.

The solid state structure of ***exo*-2b**−**B$_1$** confirms the presence of a bulky $-CH_2SiMe_2CH_2SiMe_3$ group in the

(32) The ROESY pulse sequence was more effective than the NOESY experiment for these relatively high molecular weight ion pairs: *Two-Dimensional NMR Spectroscopy: Applications for Chemists and Biochemists*, 2nd ed.; Croasman, W. R., Carlson, R. M. K., Eds.; VCH Publishing Inc.: New York, 1994; pp 329−341.

(33) It should be noted that in an earlier paper we assigned the isomers of the unsymmetrically alkylated complex $L^{tBu}Sc(CH_3)CH_2SiMe_3$ using the assumption that the *exo* position was that giving rise to ROESY cross-peaks with the isopropyl methine signals. Thus, using the present analysis, that original assignment was probably incorrect and the major isomer in this neutral compound has the methyl group in the *endo* position.

Scheme 4

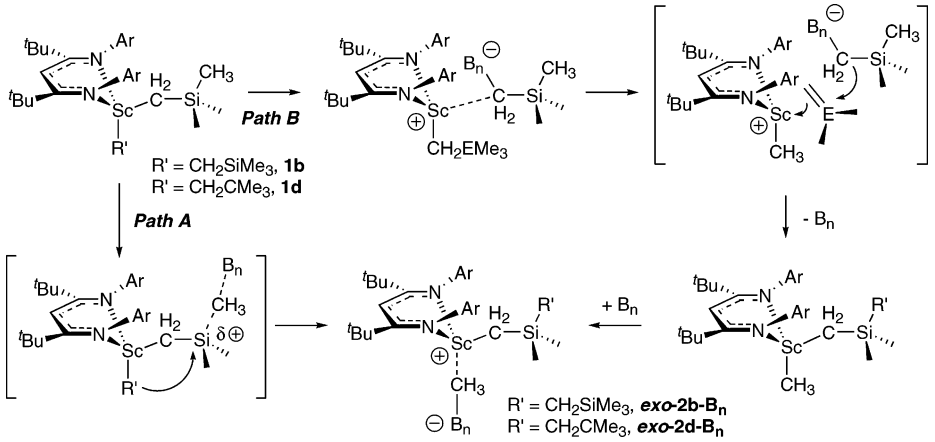

exo coordination site and exhibits several noteworthy metrical parameters. The Sc−C1 bond distance of 2.499(3) Å is significantly elongated from the typical 2.20 Å observed in the neutral starting materials, but is shorter than the analogous distance observed in either $[L^{Me}Sc(C_6F_5)]^+[MeB(C_6F_5)_3]^-$ or ***endo*-2a−B$_1$**. Because the methylborate anion occupies the more sterically hindered *endo* site, it assumes a more typical linear Sc−C1−B contact (176.8(2)°) with the scandium cation. The inability of the anion to flex and electronically stabilize the metal center through an Sc−F interaction results in a more Lewis acidic metal center, thus drawing the methylborate anion closer. The steric impact of the $-CH_2SiMe_2CH_2SiMe_3$ alkyl is apparent in the Sc−C2−Si1 bond angle of 144.47(15)°, which is opened considerably from the ideal tetrahedral value of 109.5°. That this structure is maintained in solution is supported by a ^{1}H−^{1}H 2D-ROESY NMR experiment, which shows a distinct cross-peak between the downfield isopropyl methane resonance (the "lower" isopropyl, see **II**) and the CH_3 group of the methyl borate anion; no cross-peaks between the isopropyl and alkyl groups are observed.

Two reasonable mechanisms for the formation of ion pairs ***exo*-2b−B$_n$** are depicted in Scheme 4. Path A has been proposed to operate in similar couplings observed in early metal chemistry bis(trimethylsilyl) compounds[34] and involves borane abstraction of a methyl group from a silicon center in the CH_2SiMe_3 group; as the positive charge develops on Si, it is quenched by transfer of the other Sc-R′ group to form the coupled alkyl ligand and the methylborate counteranion directly. The other invokes direct abstraction of the entire CH_2SiMe_3 from scandium by the boranes, yielding an intermediate ion pair which can undergo β-methyl elimination[22,35] from the remaining alkyl group. The eliminated isobutylene or dimethylsilene then undergoes attack by the $[Me_3SiCH_2B(C_6F_5)_3]^-$ anion to generate the neutral dialkyl shown, which reacts immediately with the **B$_n$** to yield the products. Although this mechanism has some precedence in the decomposition of some $L_2Pt(CH_2SiMe_3)_2$ compounds,[36] and borane abstraction of entire CH_2SiMe_3 groups has been observed in some instances,[37] we currently favor path A. This mechanism more readily accommodates the observations that the bis-neopentyl complex **1c** does not react at all with the boranes **B$_1$** or **B$_2$**[38] and that reaction of the mixed alkyl species **1d** with **B$_1$** exclusively produces the ion pair ***exo*-2d−B$_1$**, in which the neopentyl group migrates to the silicon atom. Furthermore, for path B, observation of intermediate ion pairs and small amounts of isobutylene and/or $H_2C{=}SiMe_2$ decomposition products might be expected; none of these species were observed in these reactions.

As mentioned above, $-C_6F_5$ transfer from the anion to the scandium center is not a feature of the ion pairs formed when using L$^{t\mathrm{Bu}}$. The greater steric presence of this ligand is enough to discourage this decomposition mode; however, as in the neutral dialkyl systems, these compounds are prone to metallative loss of RH to form an *endo*/*exo* mixture of the compounds **4**−**B$_n$** (Scheme 5). The progress of these reactions was conveniently followed using ^{19}F and ^{1}H NMR spectroscopy and were found to proceed first order in the concentration of ion pair.[39] The observed rate constants for metalation in ion pairs **2a**−**B$_n$** and ***exo*-2b**−**B$_n$** at 308 K are collected in Table 1. Representative rate constants for metalation

Scheme 5

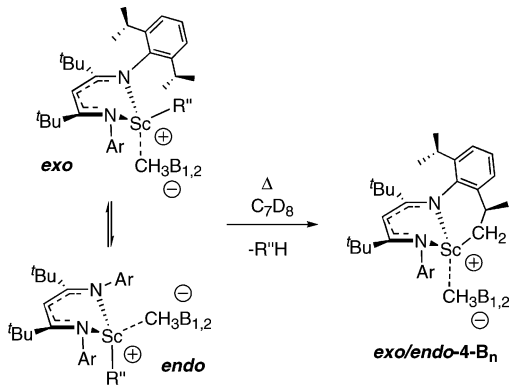

R'' = Me, ***exo/endo*-2a-B$_n$**
R'' = $CH_2SiMe_2CH_2SiMe_3$, ***exo*-2b-B$_n$**
R'' = $CH_2SiMe_2CH_2CMe_3$, ***exo*-2d-B$_n$**

(34) (a) Gielens, E.; Tiesnitsch, J. Y.; Hessen, B.; Teuben, J. H. *Organometallics* **1998**, *17*, 1652. (b) Cameron, T. M.; Gordon, J. C.; Michalcyzk, R.; Scott, B. L. *Chem. Commun.* **2003**, 2282.

(35) Hajela, S.; Bercaw, J. E. *Organometallics* **1994**, *13*, 1147.

(36) Ankianiec, B. C.; Christou, V.; Hardy, D. T.; Thomson, S. K.; Young, G. B. *J. Am. Chem. Soc.* **1994**, *117*, 9963.

(37) Arndt, S.; Spaniol, T. P.; Okuda, J. *Chem. Commun.* **2002**, 896.

(38) Abstraction of a methyl group from a carbon atom by a perfluoroaryl borane has no precedent to our knowledge and is probably kinetically and thermodynamically disfavored.

(39) Representative ^{19}F NMR spectra, first-order plots, and the Eyring plot are included as Supporting Information.

Scheme 6

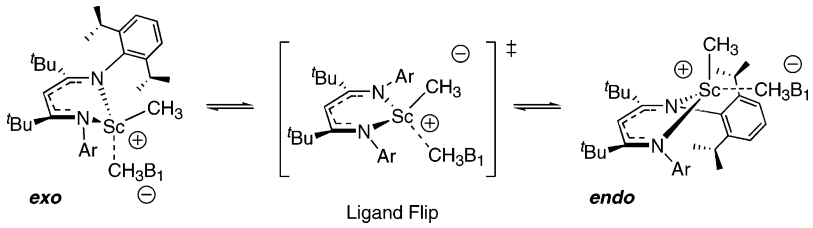

Table 1. Half-Lives and k_{exp} for Metalation Reactions

cmpd	temp (K)	$t_{1/2}$ (h)	k_{exp} (s^{-1})
	Ion Pairs		
2a−**B$_1$**	308	1.83	$1.05(2) \times 10^{-4}$
2a−**B$_2$**	308	1.32	$1.46(2) \times 10^{-4}$
2b−**B$_1$**	308	1.97	$9.77(3) \times 10^{-5}$
2b−**B$_2$**	308	7.70	$2.50(3) \times 10^{-5}$
2b−**B$_1$**	308	2.0	$1.02(3) \times 10^{-4}$
2b−**B$_1$**	308	2.0	$9.77(3) \times 10^{-5}$
2b−**B$_1$**	313	1.2	$1.67(2) \times 10^{-4}$
2b−**B$_1$**	318	0.6	$3.00(2) \times 10^{-4}$
2b−**B$_1$**	323	0.4	$5.53(3) \times 10^{-4}$
	Neutral Compounds		
1a	308	12.26	$1.57(3) \times 10^{-5}$
1b	308	17.99	$1.07(2) \times 10^{-5}$

in the neutral analogues **1a** and **1b** are also included for comparison. The metalation of ***exo*-2b**−**B$_1$** was followed at various temperatures, and an Eyring plot[39] yielded the activation parameters $\Delta H^{\ddagger} = 21.5(2)$ kcal mol^{-1} and $\Delta S^{\ddagger} = -7.0(7)$ eu. The enthalpic barrier is similar to that observed for the neutral analogues (cf. 19.7(6) kcal mol^{-1}), but the entropy of activation, while still negative, is significantly lower in magnitude (cf. −17(2) eu). This can likely be attributed to the enhanced spatial freedom of the weakly coordinating $[MeB(C_6F_5)_3]^-$ anion in the σ-bond metathesis transition state.

As can be seen from the data in Table 1, the measured rates of metalation for the various ion pairs were approximately an order of magnitude greater than those determined for the neutral dialkyl species, with half-lives of 1−2 h at 35 °C. Although the rate of metalation in the methyl cations incorporating **B$_1$** and **B$_2$** were similar, curiously, ***exo*-2b**−**B$_2$** was significantly more resistant to metalation that the $B(C_6F_5)_3$ derivative ***exo*-2b**−**B$_1$**. In any case, the rates of this process are generally quite slow, in keeping with the general observation that σ-bond metathesis reactions[40] (even intramolecular ones) are not prominent in non-Cp* scandium complexes. For example, we have never observed C−D bond activation of solvent molecules, and even reactions of the L^RScR_2 compounds with H_2 are slow.[41] This has been attributed to more ionic character in the L−Sc bonding, giving rise to retracted d-orbitals that are less available for interaction with C−H σ-bonds.[42] This is perhaps fortunate, in that the ion pairs **2** are stable enough toward metalation that detailed studies concerning the ion pair dynamics associated with these compounds could be performed.

(40) (a) Thompson. M. E.; Baxter, S. M.; Bulls, A. R.; Burger, B. J.; Nolan, M. C.; Santarsiero, B. D.; Schaefer, W. P.; Bercaw, J. E. *J. Am. Chem. Soc.* **1987**, *109*, 203. (b) Sadow, A. D.; Tilley, T. D. *J. Am. Chem. Soc.* **2003**, *125*, 7971.

(41) Hayes, P. G. Ph.D. Thesis, University of Calgary, 2004.

(42) Duchateau, R.; van Wee, C. T.; Teuben, J. H. *Organometallics* **1996**, *15*, 2291.

Dynamic Processes in Ion Pairs 2a/b−B$_n$. The existence of exchanging *exo* and *endo* isomers in the methyl cations **2a**−**B$_n$** offers an opportunity to explore the mechanism(s) of exchange via dynamic NMR spectroscopic techniques. In the present system, possible exchange mechanisms include the borane dissociation/reabstraction and ion pair reorganization mechanisms characterized by Marks and others for the metallocenium ion pairs (Scheme 1) or a simple "ligand flip" mechanism similar to what is observed in the neutral dialkyl precursors (Scheme 6). We thus probed the dynamic behavior of these CIPs, using d_8-toluene as a medium.

The complete absence of borane dissociation/reabstraction (which exchanges B-Me with Sc-Me groups) in ***exo*/*endo*-2a**−**B$_1$** on any time scale was established by the following observations. A low-temperature $^1H-^1H$ 2D EXSY experiment exhibited exchange only between the two Sc-Me signals, with no cross-peaks observed between the Sc-Me and B-Me resonances. However, B-Me/B-Me cross-peaks were also absent in this experiment, probably due to quadrupolar broadening from the boron atoms, and so to unambiguously ascertain if this process was taking place on the chemical time scale, the deuterium labeling experiment depicted in Scheme 7 was conducted. The dicationic compound **3a**−**B$_1$** was treated with d_6-**1a**, labeled selectively in the Sc-Me positions, producing 2 equiv of d_3-***exo*/*endo*-2a**−**B$_1$**. While the kinetic product of this reaction would be expected to incorporate the deuterium label only in the Sc-Me position, if borane dissociation/reabstraction were occurring, the label should wash into the B-Me sites, while unlabeled Me groups should

Scheme 7

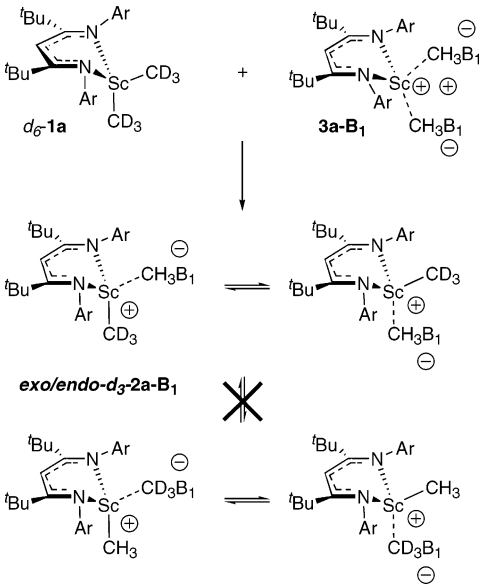

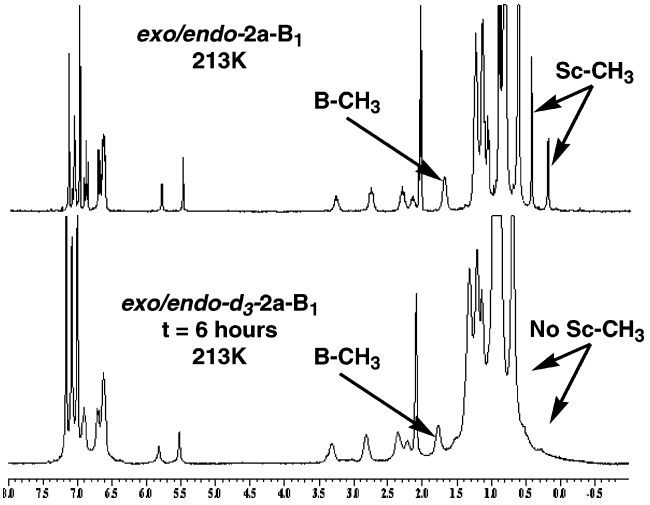

Figure 5. Top: 400 MHz ^{1}H NMR spectrum of ***exo/endo*-2a−B$_1$** at 213 K for comparison to Bottom: 400 Hz ^{1}H NMR spectrum of selectively labeled ***exo/endo*-d_3-2a−B$_1$** at 213 K after 6 h, with periodic (hourly) warming to room temperature for 5−10 min. No exchange of CH_3 groups into the Sc-Me positions is observed.

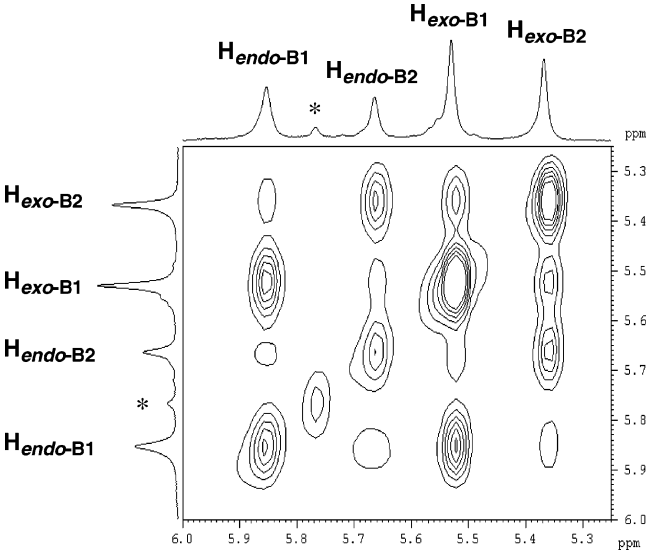

Figure 6. 400 MHz ^{1}H−^{1}H EXSY NMR spectrum for a 1:1 mixture of ***exo/endo*-2a−B$_1$** and ***exo/endo*-2a−B$_2$** at 213 K, focusing on the region where the CH proton of the β-diketiminato ligand resonates. The peak marked with (*) is likely due to a small portion of μ-methyl dimer (see ref 20b) since samples were generated with a slight deficit of $B(C_6F_5)_3$; it constitutes less than 5% of the total [Sc] and is not involved in the exchanges observed by this experiment.

materialize in the Sc-Me groups. As can be seen in Figure 5, signals for the Sc-Me groups in ***exo/endo*-2a−B$_1$** are nearly completely absent[43] in this sample, even after 6 h, wherein the sample had been warmed to RT periodically. Clearly then, this process does not occur in these ion pairs even on the chemical time scale. Since the facility of borane dissociation/reabstraction has been related to the relative magnitudes of the M−Me and B−Me bond strengths,[11] this observation implies that the Sc−CH_3 bonds in **1a** are somewhat weaker than those in the zirconocenium and hafnocenium ions where this process is observable, a notion further supported by the observed ease with which a second Sc-Me group is abstracted from these cations.

Although these experiments determined it should be possible to study ion pair symmetrization in the absence of borane dissociation/reabstraction, the **2a** system is complicated by the fact that it is possible to exchange the ***exo*** and ***endo*** isomers via a ligand flip process (Scheme 6) as well as an ion pair reorganization mechanism. In an attempt to deconvolute these processes, ion exchange between the *exo*/*endo* ion pairs differentiated by the borane **B** employed was studied. Thus, a 1:1 mixture of ***exo/endo*-2a−B$_1$** and ***exo/endo*-2a−B$_2$** in d_8-toluene was cooled to a temperature regime where *exo*/*endo* exchange was slow on the NMR time scale and studied via ^{1}H−^{1}H EXSY spectroscopy.[44] By observing exchange within each ion pair versus exchange between each ion pair, we hoped to differentiate between the ligand flip (intramolecular) and the ion pair reorganization process (potentially intermolecular). The experiment is depicted in Scheme 8, and it is assumed that the properties described above for ***exo/endo*-2a−B$_1$** also apply to the **B$_2$** ion pair. As can be seen in Figure 6, the signals for the backbone proton of the β-diketiminato ligand are baseline resolved for all four of the isomers/compounds present in this mixture at low temperature (213 K). The EXSY map in Figure 6 also shows that all four isomers are exchanging with each other under these conditions. At the same mixing time, however, the cross-peaks for exchange *within* the ion pairs are more intense than those that arise from exchange *between* the ion pairs, suggesting qualitatively that the ligand flip process is faster than intermolecular ion pair reorganization.

Scheme 8

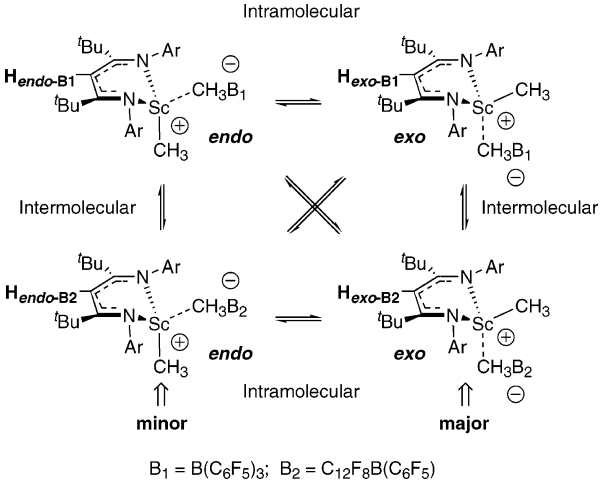

Rate constants for the various exchanges manifested in the EXSY spectrum of Figure 6 can be obtained via analysis of the volumes of the cross-peaks as a function of mixing time using an equation that accounts for the fact that the *exo* and *endo* isomers are present in about a 2:1 ratio.[44] The EXSY experiments can be performed at various temperatures allowing for analysis of the thermodynamic parameters associated with each exchange. These data are collected in Table 2, while a

(43) Close inspection reveals that a small amount (~1−2%) of Sc-CH_3 is present at the beginning of the experiment; the amount does not change over time, and we attribute this to a small amount of unlabeled material present in the d_6-**2a−B$_1$** starting material.

(44) Perrin, C. L.; Dwyer, T. J. *Chem. Rev.* **1990**, *90*, 935.

Table 2. Kinetic and Thermodynamic Data for Exchange between *exo/endo*-2a−B_1 and *exo/endo*-2a−B_2 (intermolecular, entries 1−4; intramolecular, entries 5−6) and *exo*-2b−B_1 and *exo*-2b−B_2 (entry 7)

entry	exchange partners		T (K)	k_{exp} (s^{-1})	$\Delta H^{\ddagger}$ (kcal mol^{-1})	$\Delta S^{\ddagger}$ (eu)
1	***exo*-2a−B_1**	***exo*-2a−B_2**	222.7	0.52(1)	10.5(3)	−12(1)
			228.0	0.73(2)		
			233.4	1.68(2)		
			238.7	2.50(2)		
2	***exo*-2a−B_1**	***endo*-2a−B_2**	222.7	0.51(1)	11.6(3)	−7(1)
			228.0	0.80(1)		
			233.4	1.67(1)		
			238.7	3.04(3)		
3	***endo*-2a−B_1**	***exo*-2a−B_2**	217.3	0.23(1)	11.8(2)	−7(1)
			222.7	0.50(1)		
			228.0	0.73(1)		
			233.4	1.59(3)		
			238.7	3.00(3)		
4	***endo*-2a−B_1**	***endo*-2a−B_2**	217.3	0.37(1)	11.0(2)	−9(1)
			222.7	0.78(2)		
			228.0	1.27(1)		
			233.4	2.40(3)		
			238.7	4.19(4)		
5	***endo*-2a−B_1**	***exo*-2a−B_1**	217.3	0.68(2)	13.2(2)	2(1)
			222.7	2.30(3)		
			228.0	4.03(4)		
			233.4	7.12(6)		
			238.7	12.60(9)		
			244.0	26.9(2)		
6	***exo*-2a−B_2**	***endo*-2a−B_2**	217.3	0.63(1)	13.2(3)	2(1)
			222.7	2.02(2)		
			228.0	3.18(3)		
			233.4	5.82(6)		
			238.7	9.95(9)		
			244.0	26.7(2)		
7	***exo*-2b−B_1**	***exo*-2b−B_2**	250.4	9.56(8)	8.7(3)	−20(2)
			244.0	5.20(4)		
			244.0	5.17(4)		
			244.0	5.12(4)		
			244.0	5.24(4)		
			237.0	2.57(3)		
			226.4	1.36(1)		
			221.3	0.85(1)		
			217.1	0.50(1)		

representative Eyring plot (for the data concerning exchange between ***endo*-2a−B_1** and ***endo*-2a−B_2**, entry 4) is given in Figure 7.

As can be seen, the $\Delta S^{\ddagger}$ for the exchange processes *between* the ions are negative in all cases, with the magnitude varying from −7(1) to −12(1) eu at 0.0197 M. On the other hand, the $\Delta S^{\ddagger}$ values for intramolecular exchange between isomers with the same anion (***exo/endo*-2a−B_1** and ***exo/endo*-2a−B_2**, entries 5 and 6, Table 2) are close to zero, with values similar to that

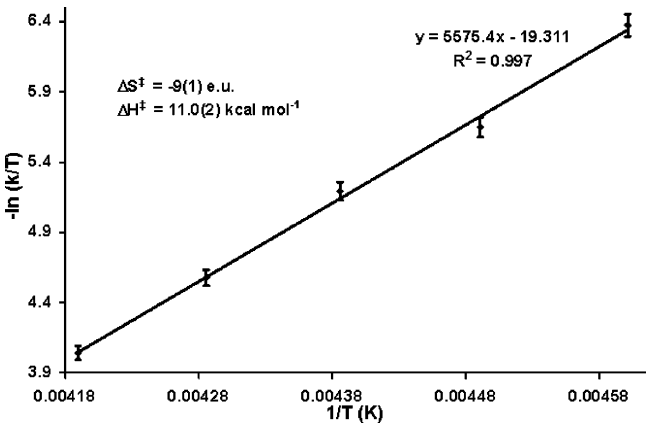

Figure 7. Eyring plot of intermolecular exchange between ***endo*-2a−B_1** and ***endo*-2a−B_2** (Table 2, entry 4).

observed for the ligand flip process in the neutral dialkyl derivative $L^{tBu}Sc(CH_2SiMe_3)_2$, **1b** ($\Delta H^{\ddagger}$ = 12.9(2) kcal mol^{-1}, $\Delta S^{\ddagger}$ = −1.6(5) eu). This observation, along with 4-fold rate enhancements for these exchanges relative to the intramolecular examples, suggests that the ligand flip process is the dominating exchange mechanism in these situations. The $\Delta H^{\ddagger}$ are similar for all of the exchange pathways with values ranging from 10.5 to 11.8 kcal mol^{-1}, suggesting that the differences in the rates are entropically driven.

The negative entropies of activation for the exchanges between isomers of **2a−B_1** and **2a−B_2** are suggestive of a mechanism with a rate-limiting step that is associative in character, although the values are generally fairly low. Attempts to ascertain the effect of varying [Sc] on the rates of exchange were unsuccessful due to the narrow range of concentrations accessible under these conditions and a threshold concentration ($\approx 1.5 \times 10^{-2}$ M) necessary to obtain reliable rate data from an EXSY experiment over a manageable time frame. Since the $\Delta S^{\ddagger}$ values could be influenced by the ligand flip process found in these scandium methyl cations, we decided to explore the intermolecular exchange process in ion pairs **2b−B_n** and **2d−B_n**, in which only the *exo* isomer is observed and presumably intramolecular ligand flip processes are suppressed relative to intermolecular ion exchange. That ion promiscuity is also a

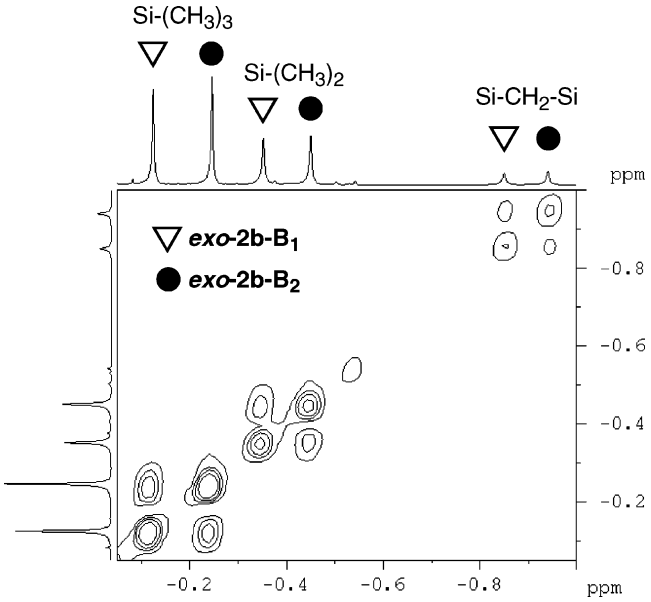

Figure 8. ^{1}H−^{1}H EXSY NMR spectrum of ***exo*-2b−B$_1$** and ***exo*-2b−B$_2$**.

characteristic of these ion pairs was demonstrated qualitatively by mixing ***exo*-2b−B$_2$** and ***exo*-2d−B$_1$** in a 1:1 ratio and recording the ^{1}H NMR spectrum, which showed a statistical mixture of all four possible ion pairs (i.e., ***exo*-2b−B$_1$** and ***exo*-2d−B$_2$** were present as well) upon mixing. This was demonstrated by computationally summing the ^{1}H NMR spectra of the four individual ion pairs and comparing the result to the spectrum of the mixture; there was excellent agreement between the two spectra (see Figure S3).

This qualitative experiment was followed up with a quantitative study involving the observed exchange between the alkyl groups in the ion pairs ***exo*-2b−B$_1$** and ***exo*-2b−B$_2$** via ^{1}H−^{1}H EXSY experiments (Figure 8, Table 2, entry 7). In these ion pairs, the signals for the two backbone protons were not baseline resolved at 400 MHz, and so the signals for the $SiMe_2$, $SiMe_3$, and $SiCH_2Si$ protons were used to assess the rate of exchange; this allowed for an internal check on the precision of the data, and the values obtained at 244 K in Table 2 reflect rate constants obtained from the different resonance pairs as labeled in Figure 8. From EXSY experiments run at various temperatures, an Eyring plot was obtained (see Figure S4), and the thermodynamic parameters given in Table 2, entry 7, were obtained. The activation parameters ($\Delta H^{\ddagger} = 8.7(3)$ kcal mol^{-1}, $\Delta S^{\ddagger} = -20(2)$ eu) differ substantially from those obtained for the intermolecular ion exchanges observed between the scandium methyl ion pairs. In particular, the entropy of activation is significantly more negative, while the activation enthalpy is lower by 2−3 kcal mol^{-1}.

Taken together, these results may be interpreted in terms of a two-step mechanism that involves reversible (and rate limiting) associative solvation of the CIPs to form solvent-separated ion pair (SSIP) intermediates that can undergo rapid exchange of ions before collapsing back to a CIP mixture in which the ions have been statistically randomized (Scheme 9). The negative $\Delta S^{\ddagger}$ values are consistent with associative displacement of the methylborate anions by solvent, in this case toluene. In the ion pairs ***exo*-2b−B$_n$**, the values are more negative and reflective of the intrinsic entropy of activation for this process, while in the ***endo*/*exo*-2a−B$_n$** ion pairs, ligand flipping attenuates the observed value because of the higher flexibility of this system. The $\Delta H^{\ddagger}$ values are lower in the **2b** ion pairs since the much bulkier alkyl group encourages displacement of the anion from the inner coordination sphere to an outer sphere domain.

The nature of the SSIPs in Scheme 9 is supported by the isolation and characterization of a family of such species supported by the L^{Me} β-diketiminato ligand (e.g.,

Scheme 9

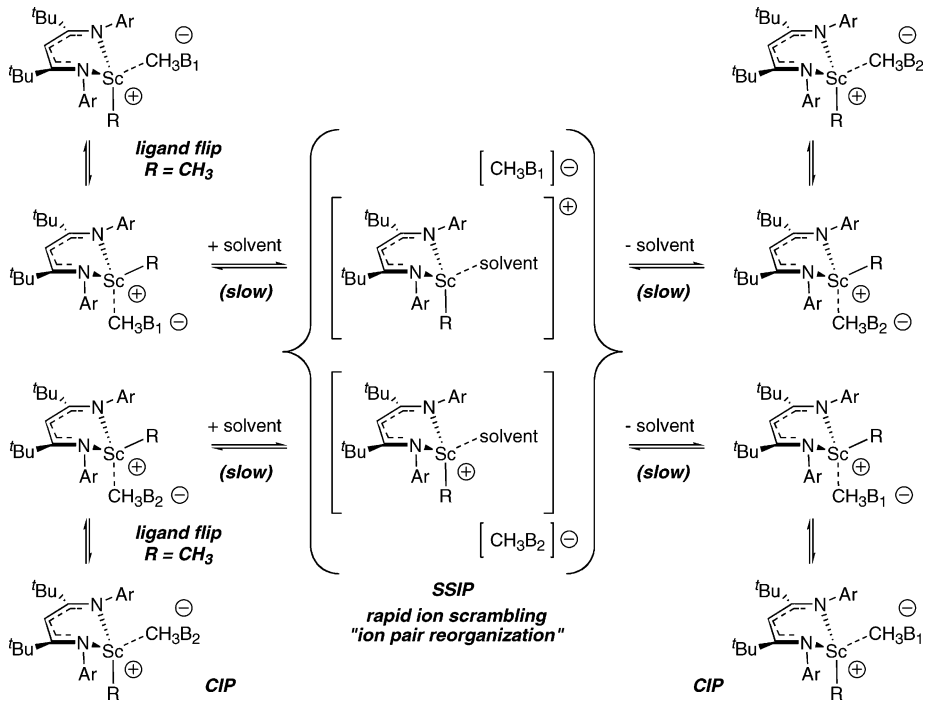

III) that we have previously reported.[21] In these com-

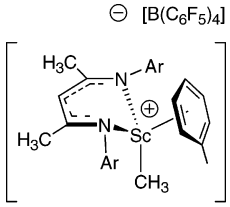

III

pounds, the arene solvents are observed to coordinate to the scandium center exclusively in the *exo* position with an unsymmetrical η^6-bonding mode and are not readily displaced by the more weakly coordinating $[B(C_6F_5)_4]^-$ anion employed. However, the coordinated arenes are in exchange with free solvent molecules, and an analysis of the activation parameters for this exchange suggests that slippage from the ground state η^6 structure to an intermediate of lower hapticity is the first step in the process.[21] In compounds **2** discussed herein, the less open coordination environment fostered by the L^{tBu} β-diketiminato ancillary and the more donating nature of the $[MeB_n]^-$ anion results in higher energies for these η^6-toluene SSIPs, but they remain viable intermediates in the present chemistry. It is possible that η^{1-4} bonding modes similar to those proposed in computational investigations of toluene-solvated metallocenium ions[45] may be operative in the SSIPs in this system. A toluene-solvated ion pair of the "constrained geometry" zirconium ion pair $[Me_2Si(C_5Me_4)(t\text{-BuN})ZrMe(toluene)]^+[B(C_6F_5)_4]^-$ has been characterized by NMR spectroscopy.[46]

That these species mediate the intramolecular ion swapping observed is supported by the recent detailed studies on the solution structures and ion pairing behavior of a variety of metallocenium CIP and SSIP derivatives by Marks et al.[12b] While not explicitly observing ion promiscuity in the same sense that we have with the crossover studies reported above, this behavior is implicit in the observed tendency of SSIPs to aggregate at moderate concentrations, while CIPs remain discrete ion pairs under all conditions studied with specific and well-defined anion−cation interactions. In the SSIPs studied, the anions were observed to be paired with the cations but were much more flexible in the position assumed about the cation environment. Further evidence in support of the involvement of SSIPs in ion mobility is found in an observation reported by Brintzinger, where rapid anion exchange between anions in the CIP $[Me_2Si(C_5H_4)_2ZrMe]^+[MeB(C_6F_5)_3]^-$ and the SSIP model $[Me_2Si(C_5H_4)_2ZrMe(NMe_2Ph)]^+[MeB(C_6F_5)_3]^-$ is "turned on" only when appreciable quantities of the SSIP are generated upon treatment of the CIP with NMe_2Ph.[8c] Whether or not formal aggregates are intimately involved in the exchange of ions between ion pairs is not clear but seems reasonable to invoke in the proper concentration regime.

(45) (a) Vanka, K.; Chan, M. S. W.; Pye, C. C.; Ziegler, T. *Organometallics* **2000**, *19*, 1841. (b) Chan, M. S. W.; Vanka, K.; Pye, C. C.; Ziegler, T. *Organometallics* **1999**, *18*, 4624.

(46) Jia, L.; Yang, X.; Stern, C. L.; Marks, T. J. *Organometallics* **1997**, *16*, 842.

Conclusions

In this paper, we have reported the synthesis and detailed solution behavior of a family of well-defined organoscandium cations with relevance to species active in olefin polymerization. To our knowledge, this is the first such study of ion pairs that are not based on the metallocenium ligand framework (or the closely related "constrained geometry" systems). The data we have acquired concerning the ion mobility within and between ion pairs add to the library of available studies concerning these important processes and support a general picture wherein intermolecular ion exchange is facile in SSIPs but not in CIPs. In ion pairs involving the relatively sticky $[MeB(C_6F_6)_3]^-$ anionic partner, the CIP is the ground state, and rate-limiting generation of a higher energy SSIP (via an associative displacement of the anion by solvent) is required to initiate rapid ion interchange. In the present study, a direct comparison between scandium methyl ion pairs **1** and ion pairs **2**, which incorporate a bulkier alkyl ligand more similar to a growing polymeryl group, reveals that ion pair reorganization is a lower energy process in compounds **2** than the methyl ion pairs **1**. This corroborates similar studies with metallocenium ions,[11] but the lower enthalpic barrier to anion displacement from the β-diketiminato scandium cations incorporating the bulky alkyl group is somewhat tempered by a higher entropic barrier due to a restriction on the fluxionality of the ancillary ligand in these more sterically crowded systems.

Acknowledgment. Financial support for this work was provided by NSERC of Canada in the form of a Discovery Grant to W.E.P. and scholarship support to P.G.H. (PGS-A and PGS-B). P.G.H. also thanks the Alberta Heritage Foundation for a Steinhauer Award and the Sir Izaak Walton Killam Foundation for a Doctoral Fellowship.

Supporting Information Available: Full experimental details, compound characterization data, representative spectra, first-order plots, and Eyring plot for the metalation of ***exo*-2b−B$_1$** and crystallographic information files (CIF) for $[L^{Me}ScMe]^+[MeB(C_6F_5)_3]^-$ and ***exo*-2b−B$_1$**. This material is available free of charge via the Internet at http://pubs.acs.org.

OM050007V